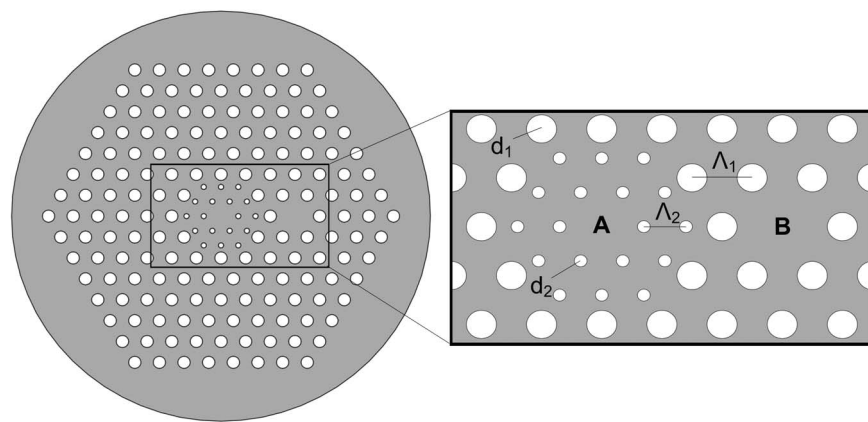


Dual-Core Photonic Crystal Fiber for Use in Fiber Filters

Volume 8, Number 2, April 2016

Haiming Jiang
Erlei Wang
Kang Xie
Zhijia Hu



DOI: 10.1109/JPHOT.2016.2539603
1943-0655 © 2016 IEEE

Dual-Core Photonic Crystal Fiber for Use in Fiber Filters

Haiming Jiang, Erlei Wang, Kang Xie, and Zhijia Hu

School of Instrument Science and Optoelectronics Engineering,
Hefei University of Technology, Hefei 230009, China

DOI: 10.1109/JPHOT.2016.2539603

1943-0655 © 2016 IEEE. Translations and content mining are permitted for academic research only.
Personal use is also permitted, but republication/redistribution requires IEEE permission.
See http://www.ieee.org/publications_standards/publications/rights/index.html for more information.

Manuscript received February 28, 2016; accepted March 5, 2016. Date of publication March 8, 2016;
date of current version March 25, 2016. This work was supported in part by the National Natural Science Foundation of China (NSFC) under Grant 60607005, Grant 60877033, Grant 11574070, and
Grant 11404087. Corresponding authors: H. Jiang, E. Wang, and K. Xie (e-mail: hmjiang@hfut.edu.cn; erlei_wang@mail.hfut.edu.cn; kangxie@hfut.edu.cn).

Abstract: An asymmetrical dual-core photonic crystal fiber (DC-PCF), which possesses all circular air holes, is proposed. By setting appropriate geometrical parameters, the wavelength-selective coupling property is realized, and a compact optical filter with a short length of 1.83 mm based on the DC-PCF is designed. The spectral transmission characteristics of the filter are investigated by the beam propagation method. The results demonstrate that the optical filter possesses a bandwidth of ~58 nm and small side-lobes. The proposed optical filter could be used in the integrated optical systems.

Index Terms: Dual-core photonic crystal fiber (DC-PCF), optical filter, transmission characteristics.

1. Introduction

Optical filters [1]–[3], which can filter unnecessary light, are widely applied in the field of modern optical systems, and they have been proposed and realized by using the conventional fibers. However, as reported in the literatures that two major disadvantages exist in the conventional fiber-based filters, i.e., the low flexibility of structure and the large size.

In recent years, photonic crystal fibers (PCFs), which possess high design flexibility and excellent light-controlling properties [4]–[15], have been widely used in the filtering fields and provide a new way to realize high performance optical filters. Based on the multi-core PCFs, Saitoh [16] designed a 78.5 mm-long bandpass filter which possesses a full width at half-maximum (FWHM) bandwidth of 3.8 nm. In order to achieve efficient broad or narrow bandpass filters, Varshney [17] proposed some design strategies and found that the characteristics of the PCF filter can be tuned by its length. In 2007, by adopting a hybrid light-guiding dual-core photonic crystal fiber, Sun [18] realized a 3.6 mm-long filters with a bandwidth of 17 nm. Then, by inserting the down-doped and up-doped silica rod in the two different cores of a PCF, Chen [19] obtained a 29 mm-long bandstop filter with a bandwidth of 26 nm and Zhou [20] achieved a 16.4 mm long filter with a narrow bandwidth of 9 nm at –3 dB loss. Recently, through filling high refractive index liquid into a PCF, Liu [21] proposed a 9-mm long multi-bandpass filter of which the wavelength range could be tuned by the temperature. With the development of modern optical communication systems toward integration and miniaturization, the compact device is more and more important. Small size is required for a fiber filter besides its optical performances. Therefore, how to reduce the length of a fiber filter has been attracting much research attention in recent years. Although the

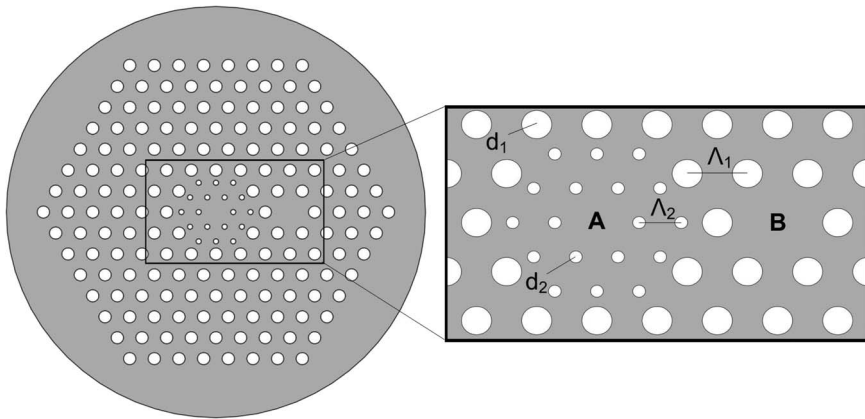


Fig. 1. Cross section of proposed DC-PCF.

fiber filters in the above-mentioned literature have their own features and advantages, their shortest length is about 3.6 mm. However, the shorter fiber filter is still needed to meet the system requirement of integration and miniaturization.

In this paper, in order to obtain a more compact optical filter, a new type of asymmetrical dual-core photonic crystal fiber (DC-PCF) which possesses all circular air holes is proposed. The wavelength-selective coupling at $\lambda = 1.55 \mu\text{m}$ is implemented by setting appropriate geometrical parameters. By adopting the beam propagation method (BPM) [22], the spectral transmission characteristics of the DC-PCF-based filter are investigated, and an optical filter with short length and small side-lobes is achieved. It could be applied widely in the development of the modern integrated optical communication systems.

2. Model and Theory

The proposed DC-PCF structure is shown in Fig. 1. The background material of the DC-PCF is pure silica (the index $n = 1.45$), as is the gray region in Fig. 1. Obviously, it possesses two parallel cores. The big air holes are arranged in triangular lattice with a hole-pitch of Λ_1 . Seven big air holes in the center are replaced by some small air holes which are also arranged in triangular lattice with a hole-pitch of Λ_2 . Core A is formed by dismissing a small air hole in the center, while core B is formed by removing a large air hole, and the distance between core A and core B is $3\Lambda_1$. The diameters of the large holes and small holes are d_1 and d_2 respectively. Because of its all circular air holes structure, this kind of PCF can be fabricated by the current technology of fiber drawing.

As is well known, the mode propagation constant β ($\beta = n_{\text{eff}}/k_0$) is an important parameter which describes transmission property of a beam, and it can be obtained by solving the electromagnetic wave equation in a PCF which can be derived from the Maxwell equations. For different fiber structures, the values of the effective refractive index n_{eff} are not equal, and therefore the propagation constants are not equal. According to the mode coupling theory, core A (B) is treated as an independent waveguide, and its property is influenced by the modal field of the other core, that is, the power can exchange between the two cores. At a certain wavelength λ , if the propagation constants of the two cores are equal, i.e., $\beta_A(\lambda) = \beta_B(\lambda)$ or the curves of n_{eff} are crossed at the wavelength of λ , the power could transfer completely between the two cores. The wavelength λ is called phase-matching wavelength (λ_{PMW}) [23]. For the symmetrical dual-core photonic crystal fiber, the propagation constants are equal at all the wavelength range, so the complete power transfer happens at any wavelength point, and it is usually used in the field of directional coupling [24], [25]. While for an asymmetrical dual-core photonic crystal fiber, there is only one wavelength which completely satisfies the phase-matching conditions, so the complete power transfer happens only at λ_{PMW} . Therefore, almost 100% power exchange

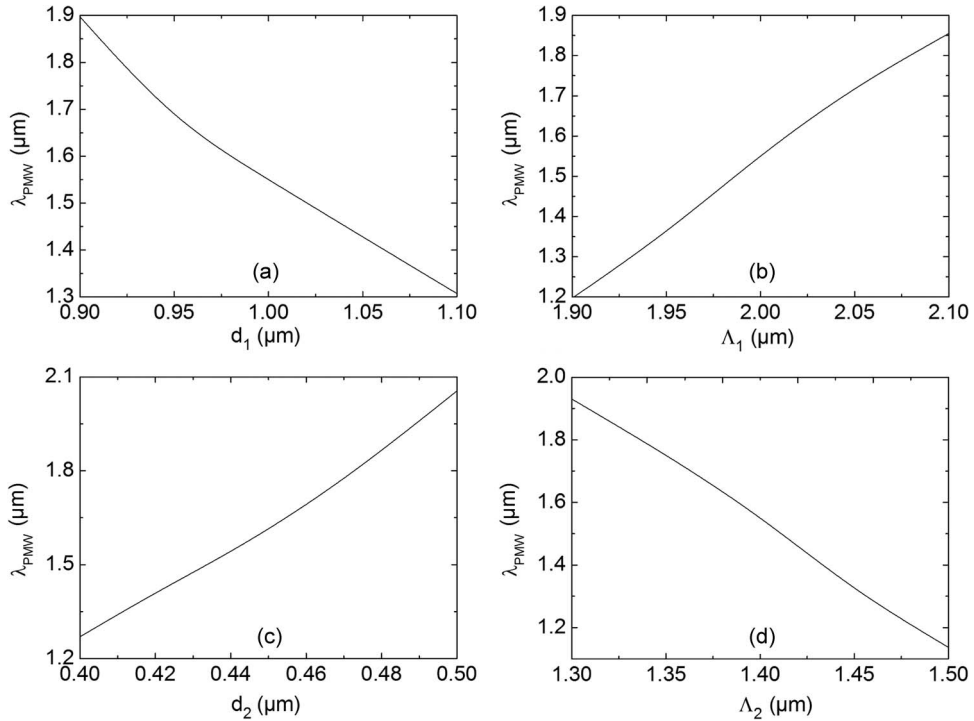


Fig. 2. Influence of geometrical parameters on λ_{PMW} . (a) d_1 , when $\Lambda_1 = 2 \mu\text{m}$, $d_2 = 0.441 \mu\text{m}$, and $\Lambda_2 = 1.4 \mu\text{m}$; (b) Λ_1 , when $d_1 = 1 \mu\text{m}$, $d_2 = 0.441 \mu\text{m}$, and $\Lambda_2 = 1.4 \mu\text{m}$; (c) d_2 , when $d_1 = 1 \mu\text{m}$, $\Lambda_1 = 2 \mu\text{m}$, and $\Lambda_2 = 1.4 \mu\text{m}$; (d) Λ_2 , when $d_1 = 1 \mu\text{m}$, $\Lambda_1 = 2 \mu\text{m}$, and $d_2 = 0.441 \mu\text{m}$.

happens between the two cores over a narrow wavelength range around the λ_{PMW} , and it can be employed in the field of bandpass/bandstop filtering. This provides the theoretical basis of the filter based on symmetrical DC-PCF. The power is transferred periodically from one core to the other, and the coupling length L [26] is defined as the periodic length. The power transfers completely between the two cores when the wavelength of the incident light is λ_{PMW} , while only part of the power transfers at the mismatched wavelength. Therefore, the filter length is defined as the coupling length (L) when the wavelength of the incident light is λ_{PMW} .

3. Results and Discussions

We hope that the power could be transferred completely between core A and core B at the communication bands, especially at the wavelength of $1.55 \mu\text{m}$, that is, λ_{PMW} is $1.55 \mu\text{m}$. Through the analysis above, there are four geometrical parameters, i.e. d_1 , Λ_1 , d_2 , and Λ_2 , need to be determined. The influence of these geometrical parameters on λ_{PMW} is studied via numerical simulations by BPM. The results are depicted in Fig. 2. The λ_{PMW} decreases with the increases of d_1 and Λ_2 , and increases with the increases of d_2 and Λ_1 . It can be seen from Fig. 2 that the λ_{PMW} is sensitive to the geometrical parameters, and therefore, we can get the fiber filters with desired working band by the adjustment of the geometrical parameters. By adjusting the geometrical parameters, the $\lambda_{\text{PMW}} = 1.55 \mu\text{m}$ can be obtained, therefore the narrowband coupling could be realized [16]. Due to the great influence of geometrical parameters on λ_{PMW} , after a large number of calculations, the geometrical parameters are as follows: $d_1 = 1 \mu\text{m}$, $\Lambda_1 = 2 \mu\text{m}$, $d_2 = 0.441 \mu\text{m}$ and $\Lambda_2 = 1.4 \mu\text{m}$. Fig. 3 shows the variation curves of the effective refractive indices at different wavelengths under the above geometrical parameters. As shown in Fig. 3, the effective refractive indices curves of core A and core B cross at $1.55 \mu\text{m}$. Like the theory in Section 2, the phase-matching condition is realized at the wavelength of $1.55 \mu\text{m}$.

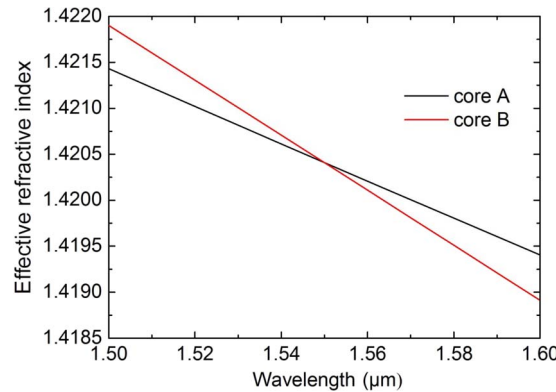


Fig. 3. Effective refractive indices of core *A* and core *B*.

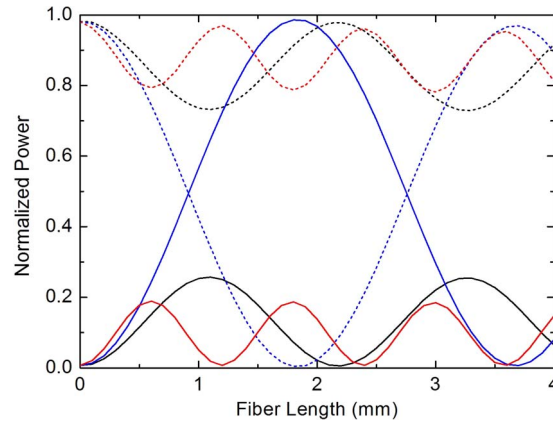


Fig. 4. Normalized output power under the incident light with different wavelengths launched in core *B*, 1.50 μm (black), 1.55 μm (blue), and 1.65 μm (red). Solid lines: Core *A*; dashed lines: Core *B*.

The BPM is adopted to calculate the coupling properties of the proposed DC-PCF. Assuming that the X-polarized light is launched in core *B* under the above geometrical parameters, the variation of normalized power with the fiber length is illustrated in Fig. 4. When the wavelengths of incident light are 1.50 μm (black), 1.55 μm (blue), and 1.65 μm (red), respectively, the output powers in core *A* are depicted as solid lines, while in core *B*, they are depicted as dashed lines. As we can see from Fig. 4, almost all of the power transfers to core *A* when the wavelength of the incident light is λ_{PMW} . However, only part of the power transfers between core *A* and core *B* at the mismatched wavelength (shown as black and red lines). Besides, the coupling lengths are also different for different incident light wavelengths. From the analysis above, the phase-matching wavelength is 1.55 μm . It validates the wavelength-selective coupling theory for an asymmetrical dual-core photonic crystal fiber. The coupling lengths for different polarizations are shown in Fig. 5, and the inset shows the partially magnified details. The coupling lengths increase with the increase of wavelength when $\lambda < \lambda_{\text{PMW}}$, while an opposite trend happens for the wavelengths of $\lambda > \lambda_{\text{PMW}}$. Although the coupling lengths are shorter at the mismatched wavelengths, the desired complete power transfer cannot be achieved at these lengths due to small power transfers of two polarizations between the two cores. However, when λ approaches λ_{PMW} , the powers transferred between the two cores increase at the cost of longer coupling lengths. When λ is right at λ_{PMW} complete power transfers are achieved. It is obvious in Fig. 5 that the

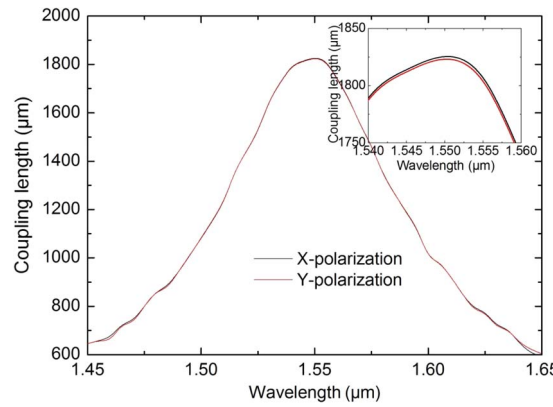


Fig. 5. Coupling length vs. the wavelength for different polarizations.

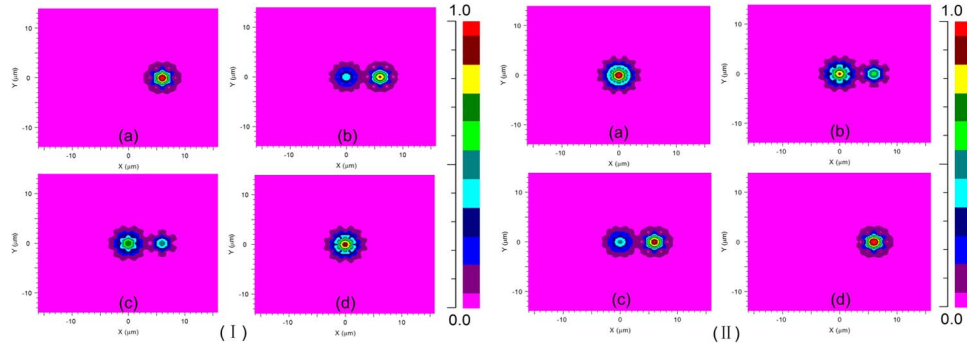


Fig. 6. Power transfer process at $\lambda = 1.55 \mu\text{m}$. (I) Launch in core B : (a) $z = 0$, (b) $z = 0.61 \text{ mm}$, (c) $z = 1.22 \text{ mm}$, and (d) $z = 1.83 \text{ mm}$. (II) Launch in core A : (a) $z = 0$, (b) $z = 0.61 \text{ mm}$, (c) $z = 1.22 \text{ mm}$, and (d) $z = 1.83 \text{ mm}$.

coupling length curve for the X -polarized state almost overlaps that of the Y -polarized state. Therefore, in the following paragraphs, only the properties for X -polarized state are presented. At the wavelength of λ_{PMW} , the coupling length of the DC-PCF is 1.83 mm, which is used as length of the fiber filter.

When the fiber length is 1.83 mm, the power transfer process of the DC-PCF is presented in Fig. 6. As illustrated in the Fig. 6 (I), when the input field is launched in core B , the power in core B transfers to core A slowly and smoothly. At the end of the fiber ($z = L$), all of the input power transfers to core A except for the power losses in the transmission process. When the input field is launched in core A , the power transfer has the same variation tendency, as shown in Fig. 6 (II); therefore, it is no more discussed in the paper. That is, the wavelength selective coupling characteristic could be realized no matter which core acts as the incident core.

From the analysis above, it can be imagined that a bandpass/bandstop filter can be realized by adopting different port as an output. When the filter acts as a bandpass/bandstop one, its performance almost remains unchanged for different input ports. Besides, the λ_{PMW} is determined by the geometrical parameters which have a great impact on the spectral characteristics. As a specific example to analyze the influence of geometrical parameters on spectral characteristics, the response of bandstop characteristics to geometrical parameters is investigated (core B acts as both input port and output port). The results are shown in Fig. 7. It can be seen that, with the increase of d_2 and \wedge_1 , the spectrum exhibits red shift, and the FWHM bandwidth increases. While the spectrum exhibits blue shift and the FWHM bandwidth decreases with the increase of

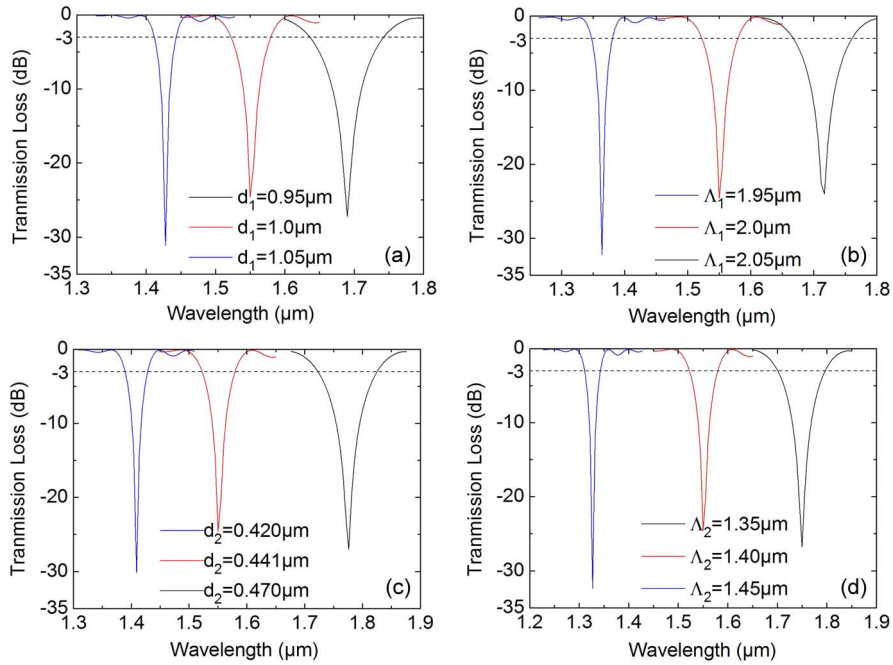


Fig. 7. Influence of geometrical parameters on the bandstop characteristics. (a) d_1 , when $\Lambda_1 = 2\text{ }\mu\text{m}$, $d_2 = 0.441\text{ }\mu\text{m}$, and $\Lambda_2 = 1.4\text{ }\mu\text{m}$; (b) Λ_1 , when $d_1 = 1\text{ }\mu\text{m}$, $d_2 = 0.441\text{ }\mu\text{m}$, and $\Lambda_2 = 1.4\text{ }\mu\text{m}$; (c) d_2 , when $d_1 = 1\text{ }\mu\text{m}$, $\Lambda_1 = 2\text{ }\mu\text{m}$, and $\Lambda_2 = 1.4\text{ }\mu\text{m}$; and (d) Λ_2 , when $d_1 = 1\text{ }\mu\text{m}$, $\Lambda_1 = 2\text{ }\mu\text{m}$, and $d_2 = 0.441\text{ }\mu\text{m}$.

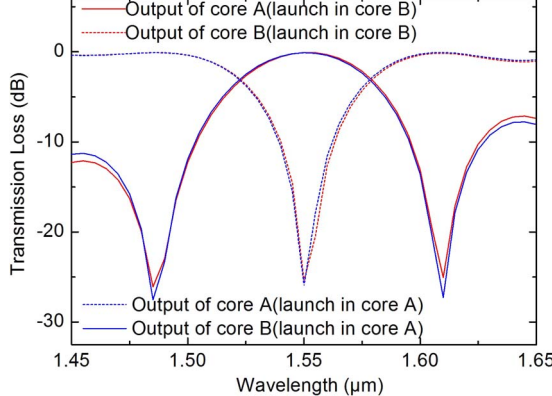


Fig. 8. Spectral characteristics of the proposed DC-PCF under $d_1 = 1\text{ }\mu\text{m}$, $\Lambda_1 = 2\text{ }\mu\text{m}$, $d_2 = 0.441\text{ }\mu\text{m}$, $\Lambda_2 = 1.4\text{ }\mu\text{m}$, and $L = 1.83\text{ mm}$.

d_1 and Λ_2 . Therefore, it is feasible to achieve the desired spectral characteristics of a fiber filter by choosing appropriate geometrical parameters.

Based on the proposed asymmetrical DC-PCF and the above discussions, a compact optical filter is proposed. The above geometrical parameters are adopted in calculating the spectral transmission characteristic of the filter. Under the conditions of the input field launches in different cores, the output powers of the two cores are shown in Fig. 8. It can be seen from Fig. 8 that the light at the phase-matching wavelength of $1.55\text{ }\mu\text{m}$ in one core is completely coupled into another core. When the input power is launched in core B, the red solid line and red dashed line represent the output powers of core A and core B, respectively. While the input power is

launched in core A , the blue solid line and blue dashed line represent the output powers of core B and core A , respectively. As shown in Fig. 8, if the input port and output port are different cores, the filter can act as a band-pass one with two small side-lobes (red solid line and blue solid line in Fig. 8). When the input port and output port are the same core, a band-stop filter can be obtained with a FWHM of ~ 58 nm, and the side-lobes are very small (red dashed line and blue dashed line). So they have very small effect on the signal transferred in the filter. In addition, when the filter acts as either a bandpass or a bandstop filter, the spectrum almost remains unchanged for different input port. Besides, the length of the filter is 1.83 mm, which is much shorter than the filter length reported in [16]–[21].

4. Conclusion

To summarize this paper, an asymmetrical dual-core photonic crystal fiber which possesses all circular air holes is used in the field of optical filters, and its performances are numerically investigated by the beam propagation method. Under the geometrical parameters of $d_1 = 1 \mu\text{m}$, $\Lambda_1 = 2 \mu\text{m}$, $d_2 = 0.441 \mu\text{m}$, and $\Lambda_2 = 1.4 \mu\text{m}$, a fiber filter with a bandwidth of ~ 58 nm, small side-lobes, and a short length of 1.83 mm is obtained, no matter which core acts as the input port. We believe that this kind of filter could be used in integrated optical systems.

References

- [1] K. Morishita, "Bandpass and band-rejection filters using dispersive fibers," *J. Lightw. Technol.*, vol. 7, no. 5, pp. 816–819, May 1989.
- [2] F. Bakhti and P. Sansonetti, "Design and realization of multiple quarter-wave phase-shifts UV-written bandpass filters in optical fibers," *J. Lightw. Technol.*, vol. 15, no. 8, pp. 1433–1437, Aug. 1997.
- [3] J. W. Yu and K. Oh, "New in-line fiber bandpass filters using high silica dispersive optical fibers," *Opt. Commun.*, vol. 204, no. 1–6, pp. 111–118, Apr. 2002.
- [4] J. C. Knight, T. A. Birks, P. S. J. Russell, and D. M. Atkin, "All-silica single-mode optical fiber with photonic crystal cladding," *Opt. Lett.*, vol. 21, no. 19, pp. 1547–1549, Oct. 1996.
- [5] J. C. Knight, T. A. Birks, R. F. Cregan, P. S. J. Russell, and P. D. de Sandro, "Large mode area photonic crystal fibre," *Electron. Lett.*, vol. 34, no. 13, pp. 1347–1348, Jun. 1998.
- [6] T. A. Birks, J. C. Knight, and P. S. J. Russell, "Endlessly single mode photonic crystal fiber," *Opt. Lett.*, vol. 22, no. 13, pp. 961–963, Jul. 1997.
- [7] N. G. R. Broderick, T. M. Monro, P. J. Bennett, and D. J. Richardson, "Nonlinearity in holey optical fibers: Measurement and future opportunities," *Opt. Lett.*, vol. 24, no. 20, pp. 1395–1397, 1999.
- [8] A. Ortigosa-Blanch *et al.*, "Highly birefringent photonic crystal fiber," *Opt. Lett.*, vol. 25, no. 18, pp. 1325–1327, Sep. 2000.
- [9] M. J. Steel and R. M. Osgood Jr., "Polarization and dispersive properties of elliptical-hole photonic crystal fibers," *J. Lightw. Technol.*, vol. 19, no. 4, pp. 495–503, Apr. 2001.
- [10] K. Suzuki, H. Kubota, S. Kawanishi, M. Tanaka, and M. Fujita, "Optical properties of a low-loss polarization maintaining photonic crystal fiber," *Opt. Exp.*, vol. 9, no. 13, pp. 676–670, Dec. 2001.
- [11] T. P. Hansen *et al.*, "Highly birefringent index-guiding photonic crystal fibers," *IEEE Photon. Technol. Lett.*, vol. 13, no. 6, pp. 588–590, Jun. 2001.
- [12] S. Kim and C.-S. Kee, "Dispersion properties of dual-core photonic crystal fiber," *Opt. Exp.*, vol. 17, no. 18, pp. 15885–15890, Aug. 2009.
- [13] M. Aliramezani and S. M. Nejad, "Numerical analysis and optimization of a dual-concentric-core photonic crystal fibers for broadband dispersion compensation," *Opt. Laser Technol.*, vol. 42, no. 8, pp. 1209–1217, Nov. 2010.
- [14] T. Fujisawa, K. Saitoh, K. Wada, and M. Koshiba, "Chromatic dispersion profile optimization of dual-concentric-core photonic crystal fibers for broadband dispersion compensation," *Opt. Exp.*, vol. 14, no. 2, pp. 893–900, Jan. 2006.
- [15] W. H. Reeves, J. C. Knight, and P. S. J. Russell, "Demonstration of ultra-flattened dispersion in photonic crystal fiber," *Opt. Exp.*, vol. 10, no. 14, pp. 609–613, Jul. 2002.
- [16] K. Saitoh, N. J. Florous, M. Koshiba, and M. Skorobogatiy, "Design of narrow band-pass filters based on the resonant-tunneling phenomenon in multicore photonic crystal fibers," *Opt. Exp.*, vol. 13, no. 25, pp. 10327–10335, Dec. 2005.
- [17] S. K. Varshney *et al.*, "Strategies for realizing photonic crystal fiber bandpass filters," *Opt. Exp.*, vol. 16, no. 13, pp. 9459–9467, Jun. 2008.
- [18] X. Sun, "Wavelength-selective coupling of dual-core photonic crystal fiber with a hybrid light-guiding mechanism," *Opt. Lett.*, vol. 32, no. 17, pp. 2484–2486, Sep. 2007.
- [19] M. Chen, Y. Zhang, and R. Yu, "Wavelength-selective coupling of dual-core photonic crystal fiber and its application," *Chin. Opt. Lett.*, vol. 7, no. 5, pp. 390–392, 2009.
- [20] J. Zhou, X.-Q. Yu, M.-Y. Chen, B. Sun, and W.-X. Jiang, "Design and characterization of a novel narrow-band filter with the dual-core photonic crystal fiber," *Optoelectron. Lett.*, vol. 6, no. 4, pp. 249–252, Jul. 2010.
- [21] Y. Liu *et al.*, "Compact tunable multibandpass filters based on liquid-filled photonic crystal fibers," *Opt. Lett.*, vol. 39, no. 7, pp. 2148–2151, Apr. 2014.

- [22] Y. Tsuji and M. Koshiba, "Adaptive mesh generation for full-vectorial guided-mode and beam propagation solutions," *IEEE J. Sel. Topics Quantum Electron.*, vol. 6, no. 1, pp. 163–169, Jan./Feb. 2000.
- [23] H. Jiang, K. Xie, and Y. Wang, "Novel asymmetrical twin-core photonic crystal fiber for gain-flattened Raman amplifier," *Sci. China Series E-Tech. Sci.*, vol. 52, no. 8, pp. 2412–2417, Aug. 2009.
- [24] J. Lægsgaard, O. Bang, and A. Bjarklev, "Photonic crystal fiber design for broadband directional coupling," *Opt. Lett.*, vol. 29, no. 21, pp. 2473–2475, Nov. 2004.
- [25] S. Lou, Z. Tang, and L. Wang, "Design and optimization of broadband and polarization-insensitive dual-core photonic crystal fiber coupler," *Appl. Opt.*, vol. 50, no. 14, pp. 2016–2023, May 2011.
- [26] H. Jiang *et al.*, "Polarization splitter based on dual-core photonic crystal fiber," *Opt. Exp.*, vol. 22, no. 25, pp. 30461–30466, Dec. 2014.